Protein Engineering of a Disulfide Bond in a β/α-Barrel Protein†

Jörg Eder‡ and Matthias Wilmanns*,§

Departments of Biophysical Chemistry and Structural Biology, Biozentrum, University of Basel, Klingelbergstrasse 70, CH-4056 Basel, Switzerland

Received November 4, 1991; Revised Manuscript Received January 31, 1992

ABSTRACT: A disulfide bond has been introduced in the β/α-barrel enzyme *N*-(5′-phosphoribosyl)anthranilate isomerase from *Saccharomyces cerevisiae*. The design of this disulfide bond was based on a model structure of this enzyme, built from the high-resolution crystal structure of the *N*-(5′-phosphoribosyl)anthranilate isomerase domain from *Escherichia coli*. The disulfide cross-link is spontaneously formed in vitro between residues 27 and 212, located in the structurally adjacent α-helices 1 and 8 of the outer helical ring of the β/α-barrel. It creates a loop of 184 residues that account for 83% of the sequence of this enzyme, thus forming a quasi circular protein. The cross-linked mutant enzyme displays wild-type steady-state kinetic parameters. Measurements of the equilibrium constant for the reduction of this disulfide bond by 1,4-dithiothreitol show that its bond strength is comparable to that of other engineered protein disulfide bonds. The oxidized, cross-linked *N*-(5′-phosphoribosyl)anthranilate isomerase mutant is about 1.0 kcal/mol more stable than the wild-type enzyme, as estimated from its equilibrium unfolding transitions by guanidine hydrochloride.

An attractive approach for the design of proteins with increased thermodynamic stability is to introduce intramolecular disulfide bonds by protein engineering methods. Disulfide cross-links can make substantial contributions to the conformational stability of a protein (Wetzel, 1987; Creighton, 1988). Therefore, disulfide bonds have been introduced by site-directed mutagenesis into T4 lysozyme (Perry & Wetzel, 1984; Matsumura et al., 1989a,b), ribonuclease H (Kanaya et al., 1991) dihydrofolate reductase (Villafranca et al., 1987), subtilisin (Mitchinson & Wells, 1989), and λ-repressor (Sauer et al., 1986). The mechanism by which disulfide bonds confer stability is not yet known in detail, but one major aspect is the decrease in entropy of the unfolded state that causes a relative stabilization of the folded conformation (Anfinsen & Scheraga, 1975; Chan & Dill, 1989; Matsumura et al., 1989a). The most substantial stabilization should be gained by connecting residues that are rather distantly located in the amino acid sequence (Pace et al., 1988; Matsumura et al., 1989a). Disulfide bonds linking N- and C-terminal regions have been shown to occur rather frequently in natural disulfide-containing proteins (Thornton, 1981).

About 10% of all proteins with known three-dimensional structure are folded as an 8-fold parallel β/α-barrel (Farber & Petsko, 1990; Brändén, 1991), first discovered for triose phosphate isomerase (Banner et al., 1975). The core of β/α-barrel proteins consists of an eight-stranded parallel β-barrel, held together by an extensive β-sheet hydrogen-bonding network. The individual β-strands are usually followed by α-helices that form an outer ring surrounding the cylindrical surface of the central β-barrel.

We have tested the idea of cross-linking a β/α-barrel enzyme with a disulfide bond on *N*-(5′-phosphoribosyl)-anthranilate isomerase from *Saccharomyces cerevisiae* (yPRAI).[1] This enzyme does not contain any disulfide bonds in its natural form. In spite of many attempts, no yPRAI crystals suitable for three-dimensional structure determination have been obtained so far. Therefore, we have modeled this structure using the high-resolution crystal structure of the PRAI domain of the bifunctional enzyme from *Escherichia coli* (ePRAI; Priestle et al., 1987; Wilmanns et al., 1992) as a template. Here we describe a mutant of yPRAI (S212C-yPRAI) that contains a single disulfide bond. The disulfide bond links two structurally adjacent α-helices together, thus yielding an almost circular protein. We show that the engineered disulfide bond forms spontaneously in vitro and stabilizes the native conformation of yPRAI.

Experimental Procedures

Materials. Dithiothreitol (DTT) and oxidized DTT were purchased from Calbiochem. Restriction enzymes were from Boehringer Mannheim Corp. The DNA-sequencing kit was from U.S. Biochemical Corp. 4-(*N*,*N*-dimethylamino)-4′-(iodoacetamido)azobenzene-2′-sulfonic acid (S-DABIA) was kindly provided by Dr. J.-Y. Chang (Pharmaceuticals Research Laboratories, Ciba-Geigy Ltd., Basel, Switzerland). Ultrapure guanidine hydrochloride (Gdn·HCl), which was used for spectroscopic studies, was purchased from Schwarz-Mann. All other reagents were of analytical grade.

Plasmids and Strains. The vector pDS56/RBSII-1 (Certa et al., 1986) was used for heterologous gene expression in the *E. coli* strain SG200-50 (Luger et al., 1989). SG200-50 is

† This work was supported in part by the Swiss National Science Foundation, Grants 31.25711.88 (to K. Kirschner) and 31.25712.88 (to J. N. Jansonius).

‡ Present address: MRC Unit for Protein Function and Design, University Chemical Laboratory, Lensfield Road, Cambridge CB2 1EW, United Kingdom.

§ Present address: Molecular Biology Institute, University of California, Los Angeles, 405 Hilgard Ave., Los Angeles, CA 90024-1570.

[1] Abbreviations: PRAI:IGPS, *N*-(5′-phosphoribosyl)anthranilate isomerase·indole-3-glycerol phosphate synthase; ePRAI, *N*-(5′-phosphoribosyl)anthranilate isomerase domain from *Escherichia coli*; yPRAI, *N*-(5′-phosphoribosyl)anthranilate isomerase from *Saccharomyces cerevisiae*; wt, wild type; DTE, 1,4-dithioerythritol; DTT, 1,4-dithiothreitol; Gdn·HCl, guanidine hydrochloride; S-DABIA, 4-(*N*,*N*-dimethylamino)-4′-(iodoacetamido)azobenzene-2′-sulfonic acid; FPLC, fast-performance liquid chromatography; HPLC, high-performance liquid chromatography; red (subscript), reduced protein; ox (subscript), oxidized protein.

0006-2960/92/0431-4437$03.00/0

```
                          <-β1>     <---α1--->   <-β2>
ePRAI    255 ...........GENKVCGLTRGQDAKAAYDAGAIYGGLIFVATSPR 289
                        |||||     |  | |  |   | | |    |
yPRAI      1 MSVINFTGSSGPLVKVCGLQSTEAAECALDSDADLLGIICVPNRKR  46

             <---α2-          -->  <-β3->     <----α3--->
ePRAI    290 CVNVEQAQEV.........MAAAPLQYVGVFRNHDIADVVDKAKVL 326
               |                   |   ||||||    ||
yPRAI     47 TIDPVIARKISSLVKAYKNSSGTPKYLVGVFRNQPKEDVLALVNDY  92

            <β4>     <---α4--->    <---β5-->
ePRAI    327 SLVAVQLHGNEEQLYIDTLREALPAHVAIWKALSVGETLPAREFQH 372
              |||||  |                                |   |
yPRAI     93 GIDIVQLHGDESWQEYQEFLGLPVIKRLVFPKDCNILLSAASQKPH 138

           <-β6->          <-α6>               <β7>    <-
ePRAI    373 VDKYVLDNGQGGSGQRFDWSLL.......NGQTLGNVLLAGGLGAD 411
                |   || |   ||                    |||||
yPRAI    139 SFIPLFDSEAGGTGELLDWNSISDWVGRQESPESLHFMLAGGLTPE 184

             --α7--- >  <-β8> <α8>       <----α8---->
ePRAI    412 NCVEAAQ.TGCAGLDFNSAVESQPGIKDARLLASVFQTLRAY      452
             |   |    | | |    ||   | ||   |
yPRAI    185 NVGDALRLNGVIGVDVSGGVETN.GVKDSNKIANFVKNAKK.      224
```

FIGURE 1: Alignment of the amino acid sequences of ePRAI (residues 255–452, above) and yPRAI (residues 1–224, below). The first and the last residues within each sequence line are numbered. The β-strands and α-helices, determined from the high-resolution structure of ePRAI, are indicated by ⟨ ⟩ and numbered above the sequence lines. Gaps are indicated by dots. Residues that are identical in the sequences of ePRAI and yPRAI are connected by vertical bars.

a *lonA*⁻ (*Tn5*) derivative of strain MC 4110 (*F*⁻, Δ *LacU169*, *araD139*, *rpsL*, *relA*, *thiA*, *flbB*) (Casabadan, 1976). Site-directed mutagenesis was performed with the expression-mutagenesis vector pMa/c5-14 and the host strains WK6 and WK6mutS (Stanssens et al., 1989).

Modeling of the yPRAI Structure and Design of the Disulfide Bond. The amino acid sequences of ePRAI (Horowitz et al., 1983) and yPRAI (Tschümper & Carbon, 1980) were aligned in consensus with 12 other PRAI sequences from different organisms (Wilmanns et al., 1992). The three-dimensional structure of yPRAI was modeled by altering the ePRAI domain of the refined PRAI·IGPS crystal structure (Wilmanns et al., 1992) on an Evans & Sutherland PS330 graphic display system using a modified version of the graphic software FRODO (Jones, 1978). Within those parts of the structure, where amino acid sequence alignments were possible, side chains of residues differing between the two homologous enzymes were exchanged. Care was taken to maintain the new side chains in the standard conformations that are provided by the program FRODO. Where strong repulsive van der Waals interactions were introduced, the conformations of side chains of replaced amino acids were interactively modified by rotations around the dihedral angles (χ_1, χ_2, etc.). The two large insertions in yPRAI, residue ranges 57–65 and 161–167 (see Figure 1), were modeled by introducing the additional amino acids and making the connection to the first aligned residue following the insertion.

The intermediate yPRAI models that resulted from the interactive modifications of the ePRAI structure were submitted to a number of energy minimization steps using the conjugant gradient algorithm of the program package X-PLOR (Brünger et al., 1987). The empirical energy function consisted of terms for covalent bond energies, bond angle energies, dihedral angle energies, and nonbonded energies, including both a van der Waals and an electrostatic energy term. The C_α-carbon atoms were restrained to their initial positions by harmonic potentials of 20 kcal/mol.

The disulfide bond between residues 27 and 212 was designed by following guidelines summarized by Matsumura et al. (1989a). The two residues to be linked together should be separated by at least 20 amino acids within the sequence, and their side-chain C_γ atoms should be closer than 6 Å in the three-dimensional model. The geometrical arrangements of residue pairs, which were potential candidates for introduction of a disulfide bond, were examined by visual inspection of the final yPRAI model on a graphic display system. Existing computer programs that search for sites where disulfide bonds can be introduced (Hazes & Dijkstra, 1988; Balaji et al., 1989) have not been used in this study.

Site-Directed Mutagenesis. Site-directed mutagenesis was performed in the vector pMc that carries an extended wild-type (wt) gene of yPRAI (Luger et al., 1990) using the gapped duplex method (Stanssens et al., 1989). Single-stranded DNA was isolated after infection with M13K07 (Walker & Gay, 1983). A 26-mer oligonucleotide (5′-GCTATTTTGTT*A*-*CA*GTCTTTTACACC-3′; sequence of the noncoding strand) was synthesized on an Applied Biosystems ABI 380B oligonucleotide synthesizer and purified by gel filtration chromatography using Sephadex G-25. This oligonucleotide substitutes a codon for cysteine (underlined) instead of serine at position 212 (S212C) by a single mismatch (italics). Mutants were selected for their resistance toward ampicillin and verified by DNA sequencing (Sanger et al., 1977) of the entire coding sequence. All other recombinant DNA techniques followed standard protocols (Maniatis et al., 1982).

Purification of Mutant yPRAI. The S212C mutant protein was purified from inclusion bodies as previously described for other yPRAI mutants (Luger et al., 1989). To prevent disulfide formation during the purification procedure, 10 mM dithioerythritol (DTE) was added to all buffers. The cells were opened by sonication at 0 °C. The pellet was dissolved in a solution of 4 M Gdn·HCl in 0.05 M potassium phosphate buffer, pH 7.5, containing 10 mM DTE and 1 mM EDTA. After centrifugation of the solution the clear supernatant was dialyzed against 10 mM potassium phosphate, pH 7.5, containing 10 mM DTE and 1 mM EDTA. The precipate was removed by centrifugation. The supernatant was loaded onto a DEAE-Sepharose fast-flow column, and the S212C mutant protein was eluted with a linear gradient of 10–250 mM potassium phosphate. The protein that was 95% pure as judged by SDS-PAGE was stored in the presence of 5 mM DTE at

−70 °C after the solution was dripped into liquid nitrogen. Typically, 15 mg of protein were obtained per liter of cell culture.

Determination of Protein Concentration. The molar concentration of yPRAI was measured by second derivative absorbance spectroscopy (Levine & Federici, 1982) using a Hewlett-Packard 8452A diode array spectrophotometer with 1-nm resolution. The molar absorptivity at 280 nm was 32000 M^{-1} cm^{-1}. At this wavelength the S212C mutant protein was assumed to have the same absorbance.

Enzyme Activity. PRAI activity was measured at 25 °C as described by Hommel et al. (1989) in 50 mM Tris-HCl at pH 7.5, in the absence or presence of DTE. Kinetic constants were determined by analyzing entire progress curves according to Duggleby and Morrison (1977).

Formation of the Disulfide Bond. Disulfide cross-linked mutant yPRAI was obtained on exposure to air during incubation in 0.1 M Tris-HCl at pH 8.0 at 4 °C for 15 h. Nonreducing SDS–PAGE (Mitchinson & Wells, 1989) as well as denaturing gel filtration chromatography has been used to assay the formation of the disulfide bond. Prior to each separation procedure, all other free cysteines were blocked by treatment with 0.1 M iodoacetamide in 0.1 M Tris-HCl at pH 8.0 at 23 °C for 2 h in the dark.

Gel filtration chromatography was performed on a Superose 12 column (1 cm × 30 cm) using a Pharmacia FPLC system. The column was equilibrated with 0.1 M Tris-HCl buffer at pH 8.0, containing 1 mM EDTA and 4 M Gdn·HCl. Elution profiles were recorded by monitoring the absorption at 280 nm after samples of 50 μL at 0.3 mg of protein/mL were injected.

Determination of Thiol Content. Free thiols were detected by titration with Ellman's reagent (Ellman, 1958) in solutions containing 4 M Gdn·HCl. In order to avoid oxidation during the removal of DTE, the reduced variant was dialyzed under a nitrogen atmosphere against a solution of 0.1 M potassium chloride and 1 mM EDTA at pH 2.0. A 0.5-mL aliquot of the oxidized or reduced protein solution was mixed with 2.5 mL of 0.1 M sodium phosphate buffer at pH 8.0, containing 5 M Gdn·HCl and 0.5 mg/mL EDTA. A total of 0.1 mL of 10 mM 5,5'-dithiobis(2-nitrobenzoic acid) in 0.1 M sodium phosphate, pH 8.0, was added immediately to 3 mL of the protein solution. The absorbance at 412 nm was measured after 15 min.

Cysteine-Peptide Mapping and N-Terminal Amino Acid Sequencing. The cysteine residues involved in the formation of the disulfide bond were identified by cysteine-peptide mapping. Prior to the labeling reaction all free thiols of the oxidized S212C mutant protein were blocked by treatment with iodoacetamide, and the disulfide bond was then reduced by addition of DTE. The resulting free cysteines were modified by reaction with S-DABIA, which is a thiol-specific, chromophoric reagent (Sun & Chang, 1989). The labeling reaction was carried out with a 10-fold excess of S-DABIA over thiol groups in 0.05 M potassium phosphate buffer at pH 7.8, containing 2 M Gdn·HCl. After incubation for 1 h at 22 ± 2 °C and subsequent removal of excess reagent by gel filtration chromatography on Sephadex G-25, the colored protein was digested with trypsin in 0.05 M ammonium bicarbonate buffer, pH 8.0, at room temperature overnight. The enzyme/substrate weight ratio was 1/20. The digested sample was directly subjected to HPLC analysis on an Aquapore RP-300 C_8 column (4.6 mm × 250 mm). Peptide fragments were eluted with a linear gradient of 0–80% acetonitrile in 15 mM sodium acetate buffer at pH 6.5. The two labeled peptide fragments were characterized by N-terminal amino acid sequencing with a gas-phase automated sequencer (Applied Biosystems 477A) according to the manufacturer's specifications.

Redox Potential of the Disulfide Bond. For determination of the stability of the disulfide bond relative to that in oxidized DTT (Wells & Powers, 1986; Matsumura et al., 1989a), S212C-yPRAI (protein concentration 18 μM) was incubated in DTT redox buffers (0.1 M Tris-HCl at pH 8.0, 0.1 mM EDTA) for 15 h at 23 °C. The ratios of $[DTT_{ox}]/[DTT_{red}]$ varied between 100 and 0.13. All solutions were degassed and saturated with nitrogen to prevent oxidation by dissolved oxygen. After incubation the samples were treated with iodoacetamide. Gel filtration in the presence of 4 M Gdn·HCl was used to separate the protein mixtures. The ratio between the reduced and oxidized S212C mutant protein was quantified using the corresponding peak areas. No change in the ratio of oxidized and reduced protein was measured after 8-h incubation.

Unfolding by Guanidine Hydrochloride. Equilibrium unfolding of wt-yPRAI and the S212C mutant protein by Gdn·HCl was monitored by following the change of circular dichroism at 222 nm (Θ_{222}) with a Cary Model 60 instrument. Oxidized and reduced enzymes were dialyzed against 0.05 M potassium phosphate buffer at pH 6.5 or pH 7.8, containing 1 mM EDTA. For the reduced S212C-yPRAI the buffers were supplemented with 1 mM DTE. The measurements were carried out on solutions of 0.1 mg of protein/mL in a cell having a 0.2-cm light path. After the protein was incubated for 3 h with the indicated concentrations of Gdn·HCl at 23 °C, Θ_{222} reached a constant value.

Results

Sequence Similarity between ePRAI and yPRAI. Figure 1 shows the amino acid sequence alignment between ePRAI and yPRAI. The sequence of yPRAI (224 residues) is longer by 26 residues than ePRAI. The difference arises from an N-terminal extension of 11 residues and two large insertions of 9 residues in the loop between α-helix 2 and β-strand 3 and of seven residues in the loop between α-helix 6 and β-strand 7. In yPRAI an insertion of one residue (L192) is compensated by a deletion of one residue between N207 and G208.

There is only 28% amino acid sequence identity between the two PRAI sequences. However, a multisequence alignment of 14 PRAI sequences and regular repeats of clusters of invariant active site residues (Wilmanns et al., 1992) permitted an unambiguous alignment except for residues 104–137 (yPRAI), which include α-helix 4 and β-strand 5. The most significant clusters of identical residues occur at the C-termini of β-strands 1, 3, 4, and 7, all part of the active site. Furthermore, the loop between β-strand 7 and α-helix 7 is involved in phosphate binding and is similar in two other enzymes of the tryptophan biosynthesis pathway, namely, indole-3-glycerol phosphate synthase and the α-subunit of tryptophan synthase (Wilmanns et al., 1991).

Three-Dimensional Model of yPRAI. The three-dimensional model of yPRAI is based on the ePRAI domain of the crystal structure of the bifunctional enzyme PRAI·IGPS, recently refined to an *R*-factor of 17.3% at 2.0-Å resolution (Wilmanns et al., 1992). The necessary side-chain replacements according to the amino acid sequence alignment were introduced into the PRAI model by a combined procedure of interactive rebuilding followed by refinement of the resulting models by energy minimization. The superimposed C_α backbones of ePRAI and yPRAI are shown in Figure 2. The overall rms deviation between the ePRAI crystal structure and the yPRAI model is 0.65 Å for 198 equivalent C_α atoms. The

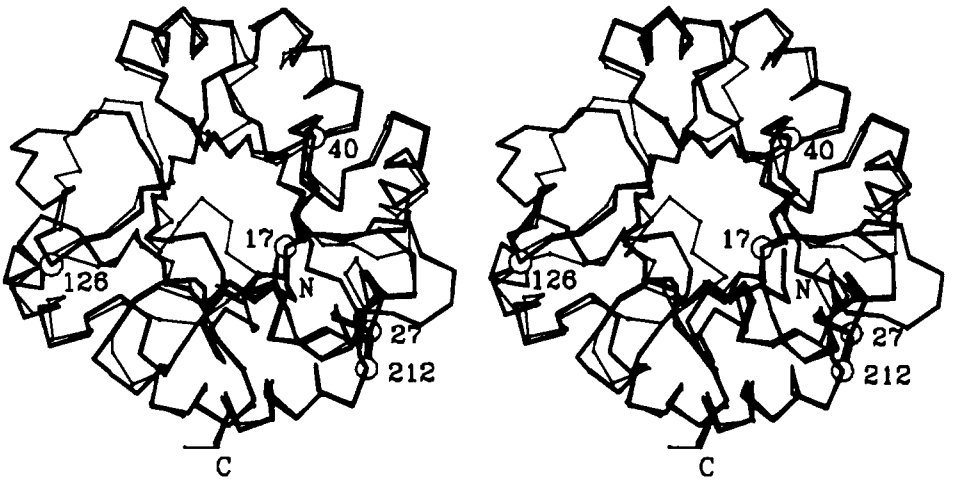

FIGURE 2: Superposition of the C_α backbones of yPRAI (thick line) and ePRAI (thin line). The view is along the barrel axis from the C-terminal side to the N-terminal side of the central β-barrel. The N-terminus and the C-terminus of the yPRAI model are labeled. The C_α positions of the four cysteines, 17, 27, 40, and 126, as well as S212 (mutated to cysteine) of yPRAI are encircled and numbered. Residues 27 and 212 are connected by a heavy line.

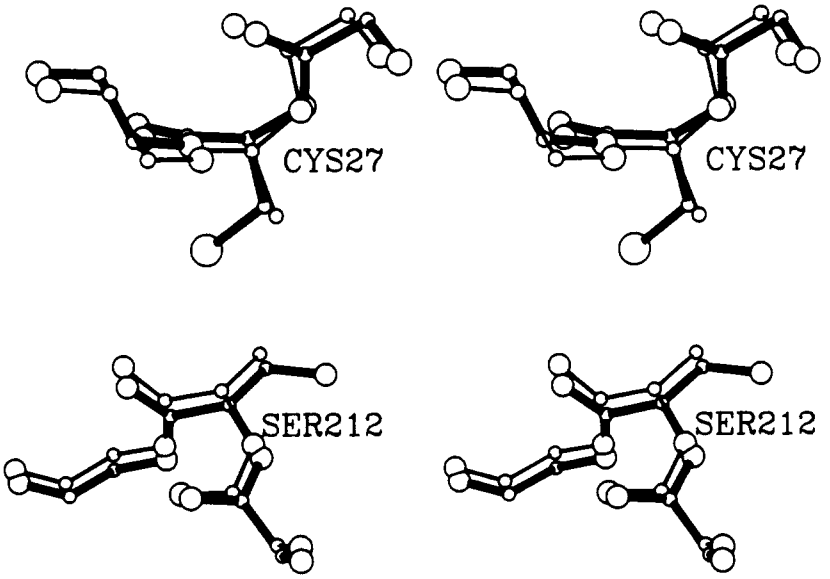

FIGURE 3: Proximity of the side chains of C27 and S212 in the yPRAI model. The tripeptides 26–28 and 211–213 of yPRAI (thick lines) are superimposed on the equivalent tripeptides 269–271 and 438–440 of ePRAI (thin lines). The side chains of the first and the last residues of each tripeptide have been omitted for clarity of the figure.

individual distances between corresponding C_α atoms do not exceed 1.5 Å.

Design of the Disulfide Bond. Residues C27 and S212 were selected for introducing a disulfide bond into yPRAI for the following reasons: (i) only introduction of one cysteine (S212C) is needed; (ii) the two residues are located in the first and the last helix of the β/α-barrel, located in adjacent positions of the outer helical ring; (iii) the two residues are located close to the N-terminus and the C-terminus of the yPRAI sequence, separated by 184 residues which account for 83% of the full length of the sequence.

The yPRAI model indicates that replacing S212 by cysteine leads to a geometrical arrangement of the two cysteine side chains that is favorable for disulfide bond formation (Hazes & Dijkstra, 1988). The C_α atoms of C27 and S212 are separated by 6.4 Å in the yPRAI model, 0.5 Å more than between the corresponding C_α atoms of A270 and A439 in ePRAI. In yPRAI the distance between the S_γ atom of C27 and the O_γ atom of S212 is only 4.4 Å because their side chains are facing each other (Figure 3).

The helix–helix interface in ePRAI, formed by A270, A271, and A274 of α-helix 1 and A439, L442, A443, and F446 of α-helix 8, is mainly of hydrophobic nature. In yPRAI residues C27, S31, and S212 are in equivalent positions as A270, A274, and A439 in ePRAI, thus forming a more polar helix–helix interface. The remaining interface residues are either identical or are replaced by similar hydrophobic amino acids. Therefore, we expected that replacement of S212 by cysteine does not significantly change the character of this helix–helix interface.

Disulfide Bond Formation. Although wt-yPRAI contains four cysteine residues (C17, C27, C40, C126; see Figure 1), the yPRAI model suggests that only a single disulfide bond between residues 27 and 212 is formed in the S212C mutant protein. In the following we provide experimental evidence that the formation of this disulfide bond is specific, spontaneous, and quantitative.

First, the remaining free thiols were measured with Ellman's reagent. Whereas 5.1 thiol groups were detected for S212C-yPRAI in its reduced state, only 3.2 thiol groups were found in its oxidized form. Under the same conditions, 4.1 and 3.8 free thiol groups were found in wt-yPRAI, respectively. These results indicate that a single disulfide bond is formed in the oxidized S212C mutant protein by the engineered C212 and one of the naturally occurring cysteines, thus decreasing the

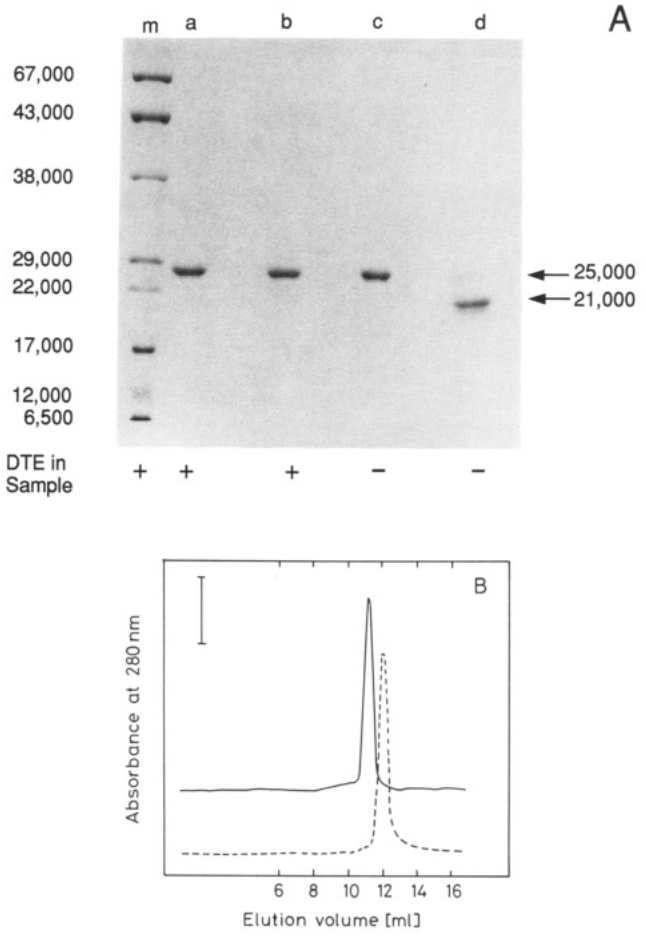

FIGURE 4: Disulfide bond formation of the S212C mutant of yPRAI. (A) 12.5% nonreducing SDS–PAGE. The presence or absence of 10 mM DTE in the sample prior to electrophoresis is indicated at the bottom of the figure. Lane m, marker proteins with indicated M_r values; lanes a and c, yPRAI; lanes b and d, S212C mutant protein. (B) Gel filtration chromatography of the S212C mutant protein in the presence of 4 M Gdn·HCl: dashed line, no DTE; solid line, 10 mM DTE. The flow rate was 0.3 mL/min. The elution profiles were monitored by measuring the absorption at 280 nm. The bar corresponds to 0.01 A_{280} unit.

number of free thiol groups by 2.

Second, the cysteine residues, which are involved in the disulfide bond, were quantitatively labeled with S-DABIA. Digestion with trypsin and subsequent HPLC analysis led to two labeled peptide fragments (V16-R44 and A211-K214). N-Terminal amino acid sequencing of these fragments showed that each contained a single S-DABIA-modified cysteine residue corresponding to C27 and C212, respectively (data not shown, but available upon request from the authors). Therefore, a single disulfide bond must have been formed in the oxidized mutant protein between residues C27 and C212.

Third, the spontaneous and quantitative formation of the disulfide bond was followed by the different mobilities of the oxidized and reduced mutant proteins in nonreducing SDS–PAGE (Figure 4A) and in gel filtration chromatography under denaturing conditions (Figure 4B). Oxidized S212C-yPRAI migrated in gel electrophoresis with an apparent M_r of 21 000 whereas its reduced form and wt-yPRAI both migrated with an apparent M_r of 25 000. The calculated M_r of wt-yPRAI is 24 583. The different mobility of the mutant forms is due to a decrease in the apparent hydrodynamic volume of the unfolded polypeptide chain upon formation of the cross-link (Pollitt & Zalkin, 1983). This decrease of the apparent hydrodynamic volume is also reflected by a difference of 1.0 mL in the elution volumes of the oxidized and the reduced S212C-yPRAI in gel filtration. Furthermore, the specific formation of the disulfide bond is underlined by the absence of any intermolecular cross-link because no dimerization was observed for the oxidized protein in both methods.

Table I: Steady-State Kinetic Constants of wt-yPRAI and S212C-yPRA1[a]

protein	DTE[b]	k_{cat} (s^{-1})	K_m (μM)	k_{cat}/K_m (μM^{-1} s^{-1})
wt-yPRAI	+	69 ± 8	3.6 ± 0.6	19
wt-yPRAI	−	70 ± 8	3.8 ± 0.6	18
S212C-yPRAI$_{red}$	+	66 ± 6	3.8 ± 0.4	17
S212C-yPRAI$_{ox}$	−	60 ± 7	3.7 ± 0.5	16

[a] The k_{cat} and K_m values were measured by spectrofluorometric assay (Hommel et al., 1989) in 50 mM Tris-HCl buffer, pH 7.5, and 4 mM EDTA, 25 °C. [b] The presence or absence of 5 mM DTE in the assay buffer is indicated by (+) or (−).

Table II: Stability of the Disulfide Bond

[DTT_{ox}]/[DTT_{red}] (mM/mM)	K_{eq}[a]	ΔG[b] (kcal mol^{-1})
19.7/0.16	7.0	−1.14
19.4/0.31	5.4	−0.99
18.7/0.63	4.9	−0.93
17.5/1.25	7.4	−1.18
15.0/2.5	3.5	−0.74
10.0/5.0	4.8	−0.92
1.25/9.4	4.0	−0.82
av value	5.3	−0.96

[a] K_{eq} is the equilibrium constant for the reduction of the disulfide bond by DTT. [b] ΔG is the free enthalpy difference, calculated according to $\Delta G = -RT \ln K_{eq}$.

Steady-State Kinetics. The engineered disulfide bond is not located in the active site of yPRAI, which is formed at the C-terminal end of the central β-barrel. Therefore, the steady-state kinetic parameters should serve as sensitive indicators for any effect on the overall structure upon formation of the disulfide bond (Table I). Both oxidized and reduced S212C-yPRAI have practically the same values of the catalytic (k_{cat}) and Michaelis (K_m) constants as wt-yPRAI. Neither the single amino acid replacement (S212C) nor the subsequent disulfide bond formation has any influence on the structural integrity of the active site of the mutant enzyme.

Stability of the Disulfide Bond. The stability of a disulfide bond can be determined from the equilibrium constant (K_{eq}) for the reduction of the enzyme (E) by DTT according to the equation

$$\Delta G = -RT \ln K_{eq}$$

with

$$K_{eq} = [E_{red}][DTT_{ox}]/[E_{ox}][DTT_{red}]$$

where ΔG is the free energy difference (Wells & Powers, 1986; Creighton, 1988; Matsumura et al., 1989a). The oxidized and reduced states of the mutant protein were separated by gel filtration chromatography after incubation with various mixtures of oxidized and reduced DTT (Figure 5). The corresponding equilibrium constants and free energy differences, calculated according to the above given equations, are summarized in Table II. The mean K_{eq} value is 5.3 ± 2.1, which corresponds to a ΔG value of −0.96 (± 0.22) kcal/mol. Therefore, the engineered disulfide bond in the S212C mutant protein is about 1.0 kcal/mol less stable than the disulfide bond in oxidized DTT.

Stability of the Mutant Protein. To estimate the net effect of the disulfide bond on the conformational stability of yPRAI, the Gdn·HCl unfolding curves of wt-yPRAI and S212C-

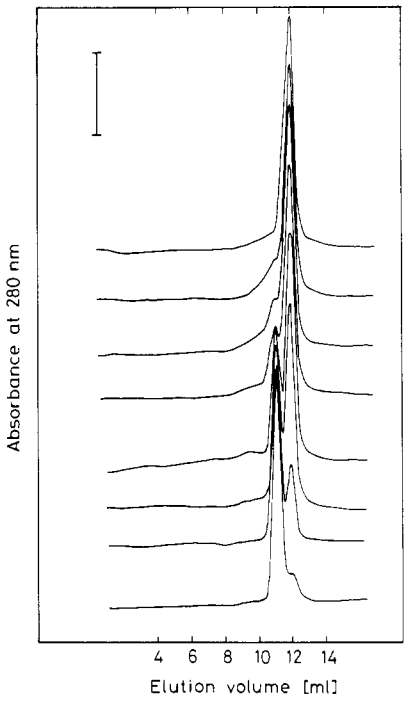

FIGURE 5: Separation of S212C-yPRAI with an intact disulfide bond (12-mL elution volume) from reduced S212C-yPRAI (11 mL) by gel filtration. The elution profiles were monitored by following the absorption at 280 nm. The bar corresponds to 0.01 A_{280} unit. The concentration ratios of DTT_{ox}/DTT_{red} (from top to bottom) are 20/0.02, 19.7/0.16, 19.4/0.31, 18.7/0.63, 17.5/1.25, 15/2.5, 10/5, and 1.25/9.4.

yPRAI were compared under both reducing and oxidizing conditions. Unfolding of yPRAI was monitored by measuring the circular dichroism at 222 nm. At this wavelength the decrease of α-helical content upon unfolding can be followed (Johnson, 1990). The respective equilibrium unfolding transition curves at pH 7.8 and pH 6.5 are shown in Figure 6. Under all conditions unfolding of wt-yPRAI and the S212C mutant enzyme was a reversible process.

At pH 6.5 the midpoints of the cooperative unfolding curves for wt-yPRAI, S212C-$yPRAI_{red}$, and S212C-$yPRAI_{ox}$ are at 0.5, 0.6, and 0.95 M Gdn·HCl, respectively (Figure 6a). Assuming that unfolding of yPRAI occurs through a two-state transition, equilibrium constants of the unfolding reaction can be calculated (Pace, 1986; Kellis et al., 1988). The slope of the free energy of unfolding as a function of the Gdn·HCl concentration is identical for all three curves (4.8 kcal mol^{-1} M^{-1}; data not shown). By comparison of the curves of S212C-$yPRAI_{ox}$ and S212C-$yPRAI_{red}$, $\Delta\Delta G_{(ox-red)}$ is estimated to be 1.0 kcal/mol, using eq 2 of Kellis et al. (1988). Only a marginal difference in stability is observed between non-cross-linked S212C-yPRAI and wt-yPRAI under identical conditions.

By contrast, at pH 7.8 the midpoints of the Gdn·HCl unfolding curves are practically identical for wt-yPRAI and S212C-yPRAI under both reducing and oxidizing conditions (about 1.1 M, Figure 6b). At this pH no apparent stabilization is provided by the disulfide bond in the S212C mutant protein. The thiol–disulfide interchange between the remaining free thiol groups of the oxidized mutant form and its disulfide bond might account for this finding. This reaction, which is reversible (Nikkel & Foster, 1971) and fast at alkaline pH (Creighton, 1988), can diminish the entropic effect on the unfolded polypeptide chain (Perry & Wetzel, 1986; Creighton, 1988). In this case it is likely that a thiol–disulfide interchange reaction would exclude a two-state folding process for the

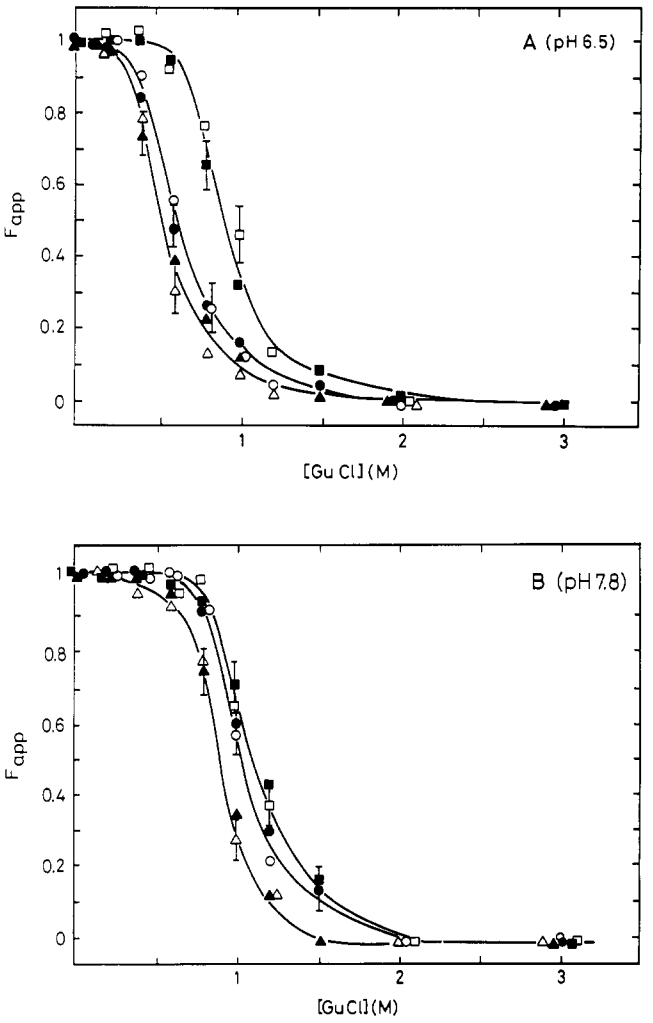

FIGURE 6: Effect of the disulfide bond on the stability of mutant yPRAI, as measured by following the Gdn·HCl-induced equilibrium unfolding/refolding curves at pH 6.5 (A) and at pH 7.8 (B). The ellipticities at 222 nm were measured as described under Experimental Procedures. The unfolding and refolding curves were normalized by extrapolating the linear change of Θ_{222} above 2 M Gdn·HCl to 0 M Gdn·HCl. The normalized change of the CD signal is the fractional deviation of F_{app} from this baseline. (▲) unfolding of wt-yPRAI; (△) refolding of wt-yPRAI; (●) unfolding of S212C-$yPRAI_{red}$; (○) refolding of S212C-$yPRAI_{red}$; (■) unfolding of S212C-$yPRAI_{ox}$; (□) refolding of S212-$yPRAI_{ox}$.

oxidized S212C-yPRAI mutant. In general, wt-yPRAI and the mutant protein are more stable at pH 7.8 than at pH 6.5.

Discussion

Structural Aspects of the yPRAI Model. The yPRAI model structure was successfully used for the design of a disulfide bond between α-helix 1 and α-helix 8. The model is judged to be reliable for the 147 (66%) residues that were unambiguously aligned to the ePRAI sequence (residues 12–66, 76–103, 138–160, 168–224). The remaining regions have also been modeled, but these parts do not necessarily represent the true three-dimensional structure of yPRAI.

All three insertions in yPRAI are located between α-helices and β-strands at the N-terminal side of the central β/α-barrel and are therefore far away from the active site. The small deletion in the loop between the additional α-helix 8′ and the C-terminal α-helix 8 is close to the phosphate binding site in ePRAI (Wilmanns et al., 1991, 1992).

The C-terminus of ePRAI (Y452) provides three hydrogen bonds to the indole-3-glycerol phosphate synthase domain of the bifunctional enzyme and participates considerably in the

interdomain interface of PRAI·IGPS from *E. coli*. The amino acid sequence of yPRAI terminates with two positively charged residues, K223 and K224. These residues presumably compensate the negative charge of the C-terminus.

In the refined ePRAI structure no helix is found between β-strand 5 and β-strand 6 (Wilmanns et al., 1992). Residue P366 of ePRAI might prevent formation of this helix. By contrast, secondary structure prediction suggests that α-helix 5 exists in yPRAI where no proline is found in the corresponding region (Niermann & Kirschner, 1991). Then I129-L130-L131 and A133-A134 of yPRAI might form the hydrophobic part of α-helix 5 that interacts with the central β/α-barrel and the adjacent α-helices 4 and 6.

Stability of the Disulfide Bond in yPRAI. The engineered disulfide bond in yPRAI is specifically, spontaneously, and quantitatively formed in vitro. Its stability was determined by estimating the free energy of the disulfide bond formation from equilibrium constants in DTT redox buffers. The C27–C212 disulfide bond is about 1.0 kcal/mol less stable than the disulfide in oxidized DTT (Table II). This value indicates a bond strength within the range observed for the most successfully engineered disulfides in subtilisin BPN′ (Mitchinson & Wells, 1989) and T4 lysozyme (Matsumura et al., 1989a), which is between +0.4 and −4.2 kcal/mol.

Both cysteines, which form the disulfide bond in S212C yPRAI, are located in α-helices. However, secondary structure often obstructs formation of disulfides (Thornton, 1981), and the most stable engineered disulfides are usually located in loop regions of the protein (Matsumura et al., 1989a). Secondary structural elements (β-strands, α-helices) tend to be more rigid than loops, thus providing less conformational flexibility for an engineered disulfide bond to adopt a geometry without serious dihedral strain. The high bond strength of the C27–C212 disulfide bond in yPRAI indicates that it can be formed without substantially changing the backbone conformation of α-helices 1 and 8.

Contribution of the Disulfide Bond to the Stability of yPRAI. At pH 6.5 the cross-linked S212C-yPRAI is about 1.0 kcal/mol more stable than the non-cross-linked form. However, other engineered disulfide bonds, e.g., in T4 lysozyme, increase the stability of the native conformation by up to 2.8 kcal/mol, if the size of the loop formed by the disulfide cross-link is large (Matsumura et al., 1989a). Conversely, the loss of naturally occurring disulfide bonds destabilizes ribonuclease T_1 by 3–4 kcal/mol per disulfide cross-link (Pace et al., 1988).

In proteins with engineered disulfide bonds the effect of a covalent cross-link on the stability does not correlate well with the reduction in entropy of the unfolded state but is offset as a result of at least two effects. Both the energetic strain of the disulfide and the disruption or loss of interactions in the native structure associated with cysteine replacements can lower the net stability of the altered protein (Creighton, 1988; Pjura et al., 1990). For the S212C mutant enzyme these two unfavorable energy contributions are expected to be very small: (i) the dihedral strain of the disulfide bond is presumably low, because the disulfide cross-link is rather stable in comparison to that in oxidized DTT, and (ii) the overall stability of non-cross-linked S212C-yPRAI is about the same as for wt-yPRAI (see Figure 6).

Taking these considerations into account, an increase in the overall stability of S212C-yPRAI of about 1.0 kcal/mol upon disulfide bond formation appears to be rather low. The theoretical equations of Pace et al. (1988) predict for a protein with a loop of 184 residues, formed by a cross-link, a net stabilization upon disulfide bond formation of about 4 kcal/mol. One explanation for the relatively small influence of the disulfide bond on the free energy of unfolding (ΔG_D) of oxidized S212C-yPRAI could be that unfolding by Gdn·HCl is not strictly a two-state transition in this case. Therefore, the calculation of ΔG_D (Pace, 1986) may not be the correct way to interpret the data. Alternatively, the presence of three other free thiols in the oxidized S212C mutant protein might decrease the entropic effect of the disulfide cross-link via thiol–disulfide interchange in the unfolded state. However, this reaction requires deprotonated thiols. Since the midpoints of the unfolding transition for cross-linked and non-cross-linked S212C-yPRAI considerably diverge with decreasing pH, it can be assumed that the disulfide interchange reaction is slowed down. However, we cannot exclude that even at pH 6.5 the interchange reaction is completely suppressed, thereby still influencing the stability of cross-linked S212C-yPRAI. Unfortunately, lower pH values cause aggregation of yPRAI, so this hypothesis could not be tested.

Conclusion

We have described the first β/α-barrel protein with an engineered disulfide bond that displays full catalytic activity and is more stable than wild-type enzyme under oxidizing conditions. The successful design of the disulfide bond indicates that the three-dimensional yPRAI model is essentially correct. A positional shift of the sequence in one of the two adjacent helices by only one residue would have introduced intolerable strain in a disulfide bond between residues 27 and 212 without affecting the integrity of the native three-dimensional fold.

The 20 β/α-barrel proteins known so far catalyze an impressive diversity of enzymatic reactions (Farber & Petsko, 1990; Brändén, 1991). Their structural backbone, in particular the central β-barrel, is usually folded in a rather rigid conformation. None of these enzymes undergo considerable conformational changes during catalysis except for the active site loop 6 (Wilmanns et al., 1991, 1992). This paper demonstrates how the native conformation of a β/α-barrel enzyme is stabilized without affecting the flexibility of the active site that is necessary for catalysis.

Acknowledgments

We thank Drs. Kasper Kirschner and Johan N. Jansonius for stimulating discussions and for their critical comments on the manuscript. We are grateful to Dr. Paul Jenö for performing HPLC analysis and N-terminal amino acid sequencing and for helpful discussions. We further thank Halina Szadkowski and Sandra Ziegler for excellent technical assistance and Dr. Jui-Yoa Chang for donating S-DABIA.

Supplementary Material Available

Data of cysteine peptide mapping and N-terminal amino acid sequencing and four figures showing the absorbance spectrum of S-DABIA-labeled S212C-yPRAI, an HPLC analysis of the tryptic digest, absorbance spectra of fractions 4 and 11, and N-terminal amino acid sequencing of the peptide fragments of fractions 4 and 11 (7 pages). Ordering information is given on any current masthead page.

References

Anfinsen, C. B., & Scheraga, H. A. (1975) *Adv. Protein Chem. 29*, 205–300.

Balaji, V. N., Mobasser, A., & Rao, S. N. (1989) *Biochem. Biophys. Res. Commun. 160*, 109–114.

Banner, D. W., Bloomer, A. C., Petsko, G. A., Phillips, D. C., Pogson, C. I., Wilson, I. A., Corran, P. H., Furth, A. J.,

Milman, J. D., Offord, R. E., Priddle, J. D., & Waley, S. G. (1975) *Nature 255*, 609–614.
Brändén, C.-I. (1991) *Curr. Opin. Struct. Biol.* (in press).
Brünger, A. T., Kuriyan, J., & Karplus, M. (1987) *Science 235*, 458–460.
Casabadan, M. J. (1976) *J. Mol. Biol. 104*, 541–555.
Certa, U., Bannwarth, W., Stüber, D., Gentz, R., Lanzer, M., Le Grice, S., Guillot, F., Wendler, I., Hunsmann, G., Bujard, H., & Mous, J. (1986) *EMBO J. 5*, 3051–3056.
Chan, H. S., & Dill, K. A. (1989) *J. Chem. Phys. 90*, 492–509.
Creighton, T. E. (1988) *BioEssays 8*, 57–63.
Duggleby, R. G., & Morrison, J. F. (1977) *Biochim. Biophys. Acta 481*, 297–312.
Ellman, G. L. (1958) *Arch. Biochem. Biophys. 74*, 443–450.
Farber, G. K., & Petsko, G. A. (1990) *Trends Biochem. Sci. 15*, 228–234.
Hazes, B., & Dijkstra, B. W. (1988) *Protein Eng. 2*, 119–125.
Hommel, U., Lustig, A., & Kirschner, K. (1989) *Eur. J. Biochem. 180*, 33–40.
Horowitz, H., van Arsdell, J., & Platt, T. (1983) *J. Mol. Biol. 169*, 775–779.
Johnson, W. C. (1988) *Annu. Rev. Biophys. Chem. 17*, 145–166.
Jones, T. A. (1978) *J. Appl. Crystallogr. 11*, 268–272.
Kanaya, S., Katsuda, C., Kimura, S., Nakai, T., Kitakuni, E., Nakamura, H., Katayanagi, K., Morikawa, K., & Ikehara, M. (1991) *J. Biol. Chem. 226*, 6038–6044.
Kellis, J. T., Nyberg, K., Šali, D., & Fersht, A. R. (1988) *Nature 333*, 784–786.
Levine, R. L., & Federici, M. M. (1982) *Biochemistry 21*, 2600–2606.
Luger, K., Hommel, U., Herold, M., Hofsteenge, J., & Kirschner, K. (1989) *Science 243*, 206–210.
Luger, K., Szadkowski, H., & Kirschner, K. (1990) *Protein Eng. 3*, 249–258.
Maniatis, T., Fritsch, E. F., & Sambrook, J. (1982) *Molecular Cloning: a Laboratory Manual*, Cold Spring Habor Laboratory Press, Cold Spring Harbor, NY.
Matsumura, M., Becktel, W. J., Levitt, M., & Matthews, B. W. (1989a) *Proc. Natl. Acad. Sci. U.S.A. 86*, 6562–6566.
Matsumura, M., Signor, G., & Matthews, B. W. (1989b) *Nature 342*, 291–293.
Mitchinson, C., & Wells, J. A. (1989) *Biochemistry 28*, 4807–4815.
Niermann, T., & Kirschner, K. (1991) *Protein Eng. 4*, 359–370.
Nikkel, H. J., & Foster, J. F. (1971) *Biochemistry 10*, 4479–4486.
Pace, C. N. (1986) *Methods Enzymol. 131*, 266–279.
Pace, C. N., Grimsley, G. R., Thomson, J. A., & Barnett, B. J. (1988) *J. Biol. Chem. 263*, 11820–11825.
Perry, L. J., & Wetzel, R. (1984) *Science 226*, 555–557.
Perry, L. J., & Wetzel, R. (1986) *Biochemistry 25*, 733–739.
Pjura, P. E., Matsumura, M., Wozniak, J. A., & Matthews, B. W. (1990) *Biochemistry 29*, 2592–2598.
Pollitt, S., & Zalkin, H. (1983) *J. Bacteriol. 153*, 27–32.
Priestle, J. P., Grütter, M. G., White, J. L., Vincent, M. G., Kania, M., Wilson, E., Jardetzky, T. S., Kirschner, K., & Jansonius, J. N. (1987) *Proc. Natl. Acad. Sci. U.S.A. 84*, 5690–5694.
Sanger, F., Nicklen, S., & Coulson, A. R. (1977) *Proc. Natl. Acad. Sci. U.S.A. 74*, 5463–5467.
Sauer, R. T., Hehir, K., Stearman, R. S., Weiss, M. A., Jeitler-Nilsson, A., Suchanek, E. G., & Pabo, C. O. (1986) *Biochemistry 25*, 5992–5998.
Stanssens, P., Opsomer, C., McKeown, Y. M., Kramer, W., Zabeau, M., & Fritz, H.-J. (1989) *Nucleic Acids Res. 17*, 4441–4454.
Sun, X.-J., & Chang, J.-Y. (1989) *J. Biol. Chem. 264*, 11288–11293.
Thornton, J. M. (1981) *J. Mol. Biol. 151*, 261–287.
Tschümper, G., & Carbon, J. (1980) *Gene 10*, 157–166.
Villafranca, J. E., Howell, E. E., Oatley, S. J., Xuong, N.-h., & Kraut, J. (1987) *Biochemistry 26*, 2182–2189.
Walker, J. E., & Gay, N. J. (1983) *Methods Enzymol. 97*, 195–218.
Wells, J. A., & Powers, D. B. (1986) *J. Biol. Chem. 261*, 6564–6570.
Wetzel, R. (1987) *Trends Biochem. Sci. 12*, 478–482.
Wilmanns, M., Hyde, C. C., Davies, R. D., Kirschner, K., & Jansonius, J. N. (1991) *Biochemistry 30*, 9161–9169.
Wilmanns, M., Priestle, J. P., Niermann, T., & Jansonius, J. N. (1992) *J. Mol. Biol. 223*, 477–507.